Molecular Cell, Volume *49*

Supplemental Information

Fbxl10/Kdm2b Recruits Polycomb Repressive Complex 1 to CpG Islands and Regulates H2A Ubiquitylation

Xudong Wu, Jens Vilstrup Johansen, and Kristian Helin

INVENTORY OF SUPPLEMENTAL INFORMATION FILE

Supplemental Experimental Procedures

7 Supplemental Figures

Figure S1 relates to Figure 1

Figure S2 relates to Figure 1

Figure S3 relates to Figure 3

Figure S4 relates to Figure 3

Figure S5 relates to Figure 3 and Figure 4

Figure S6 relates to Figure 5

Figure S7 relates to Figure 7

Supplemental References

4 Supplemental Tables

Table S1. List of ChIP-Seq Data Sets

Table S2. Fbxl10 Target Genes

Table S3. Primers and Antibodies

Table S4. Log2 Fold Change of Ring1B Binding Compared to Control ESCs on All Ring1B Target Sites, Related to Figures 5 and S6

SUPPLEMENTAL EXPERIMENTAL PROCEDURES

Cloning and Plasmid Preparation

Human and mouse FBXL10 cDNA and the different mutations were PCR-amplified from the cDNA constructs of FBXL10 from Pagano and Zhang's lab, introduced into Gateway Entry vector pCR8/GW/TOPO (Invitrogen) following the manufacturer's protocol and verified by sequencing. Different constructs were subcloned in the desired vectors by Gateway technology (Invitrogen).

RNA Interference

Specific oligonucleotides were designed and cloned into pLKO.1 TRC cloning vector according to the protocol recommended by Addgene. When required, the puromycin-selection cassette of LKO.1 vectors was exchanged with a neomycin-selection cassette by a BamHI-KpnI subcloning.

Lentivirus Transduction

All lentiviruses were generated as follows: Superfect-mediated co-transfection of lentiviral backbone with pAX8 (packaging) and pCMV-VSVG (envelope) into 293FT cells. After 48 hr, virus supernatants were column-concentrated and ESCs infected along with polybrene (8 μg/ml; Sigma). When appropriate, neomycin (0.5 mg/ml) and/or puromycin-containing media (1.5 μg/ml) was replaced 48 hr post-infection for an additional 96 hr before testing the expression.

Antibodies

Antibodies used in this study are listed in Table S3. To generate Fbxl10 antibodies, GST, GST–FBXL10 800–1000 (amino acids 800–1000 of human FBXL10) and GST–FBXL10

400-600 (amino acids 400–600 of human FBXL10) were produced in *Escherichia coli* BL21 (DE3) and affinity purified using glutathione Sepharose 4B (GE Healthcare, Piscataway, NJ). The Fbxl10 mouse monoclonal antibody was generated by immunizing mice with GST–FBXL10 800–1000 followed by fusion with hybridoma cells. The polyclonal antibody by immunizing rabbits with GST–FBXL0 400-600. The polyclonal antibodies were absorbed on GST-coupled cyanogen bromide-activated Sepharose (GE Healthcare) and subsequently affinity purified using Sepharose coupled with GST–FBXL10 400-600. Antibody specificity was confirmed by immunoblotting and immunoprecipitation.

Cell Culture, Differentiation Assays and Stable Cells Generation

293T, Flp-In T-REx 293 cells (293FT) were grown in 10% FBS (Hyclone). Stable Flp-In T-REx 293 cell lines were generated following manufacturer's instructions. To generate the Gal4-FBXL10 heterologous reporter system, subclones were made by stably expressing the shRNA construct pRS-Gal4 (puromycin selction) in the parental clone #4 (Hansen et al., 2008) (neomycin resistance) to avoid leakiness (clone #4-11). To introduce the Gal4-fusion proteins, the GAL4-FBXL10 WT or ΔLRR-pcDNA5/FRT/TO constructs were co-transfected with the pOG44 Flp recombinase into clone #4-11. Following Hygromycin B selection, clones were isolated and characterized. Positive clones with increased GAL4-fusion proteins expression in response to the tetracycline were validated by Western blotting. The cells were then expanded for further experiments.

The mouse ES cell line E14 were cultured on feeder-free on 0.1% gelatin-coated plates in 2i medium (Dulbecco's modified Eagle's medium [DMEM; Hi-Glucose]/Neuralbasel medium 1:1, non-essential amino acids, L-glutamine, b-mercaptoethanol, penicillin/streptomycin, sodium pyruvate, N2, B27 and leukemia inhibitory factor (LIF), GSK3β and MEK1 inhibitors (2i). All cell cultures were maintained at 37 °C with 5% CO2. For the differentiation assays, ES cells were cultured in LIF and the 2i-deficient ES cell medium with 10% serum for the indicated number of days. To form EBs, ES cells

were trypsinized to single-cell suspensions and cultured in uncoated Petri dishes in LIF-deficient ES cell medium for indicated number of days (Pasini et al., 2007).

Stable FH-Fbxl10 ES cell clones were generated by transfection (Lipofectamine 2000, Invitrogen) of the Fbxl10 expression constructs. Cells were selected in 2 µg/ml puromycin. For the rescue experiments, E14 cells expressing Fbxl10 shRNA from an LKO.1-neomycin vector were transfected with pCAG-ires-puro vectors expressing human FBXL10 WT, *CXXC and ΔLRR. 48 hours after transfection, the cells were selected with 2 µg/ml of puromycin while maintaining the neomycin selection. Single-cell clones were subsequently isolated.

Real-Time Quantitative PCR

For gene expression analysis, total RNA was extracted with the RNeasy Mini Kit (Qiagen) and reverse transcribed using the TaqMan® Reverse Transcription Reagents kit (Applied Biosystems). For ChIP-qPCR analysis, all quantitative PCR analyses were performed using the LightCycler® 480 SYBR Green I Master (Roche) following manufacturers' protocol on the LightCycler480 Real-Time PCR System (Roche). Each PCR reaction generated a specific amplicon, as demonstrated by melting-temperature profiles of final products (Dissociation Curve analysis). No PCR products were observed in the absence of template. In gene expression analysis, all data were normalized to *Rpo* and represented relative to a control sample (set at 1). In ChIP-qPCR analysis, data were normalized to input-DNA. Primers are listed in Table S3

Acid Extraction of Histones

Histones were purified following the Abcam protocol with minor modifications. Briefly, ESCs in the exponential growth phase were harvested and washed twice with PBS. Cell pellets were then resuspended in acid cold Triton Extraction Buffer (TEB: PBS containing 0.5% Triton X-100 2 mM PMSF, 10 µg/ml aprotinin, 10 µg/ml leupeptin) at a cell density of 10^7 cells per ml. After lysing on ice for 10 min, cells were centrifuged at 2000 rpm for 10 min at 4°C and supernatant was discarded. To remove the residual cytoplasmic protein, the cell pellets were washed one more time with the TEB buffer and

centrifuged again as before. Then the cell pellets were resuspended in 0.2N HCl at a proper density ($4x10^7$cells/ml) and vortexed overnight at 4°C. The supernatant acid extracts were collected after 10 minutes centrifugation at 6500 rpm. Then equal volume of 50% tricarboxylicacidcycle (TCA) was added and mixed on ice for 30 min. After centrifugation for 10 min at 10000 rpm, the pellets were washed with acid cold acetone and centrifuged again at 10000 rpm for 10 min. After air-drying, the pellet was resuspended in 50 mM Tris (pH 6.0). The protein concentration of the extracts was measured and aliquots were stored at -80°C until use.

Co-immunoprecipitation (CoIP) and ChIP Assay

CoIP. $3x10^7$ ES cells were scraped/trypsinized, PBS washed, swelled in hypotonic lysis buffer (10 mM HEPES ph 7.9, 1.5 mM $MgCl_2$, 10 mM KCl, 1 mM DTT, protease inhibitors) and disrupted by using a syringe with a narrow-gauge hypodermic needle. After centrifugation, the nuclei pellet was lysed in IP 300 Buffer as described (Pasini et al., 2008), pre-cleared and incubated overnight with 5 µg antibody, and captured with Protein A or Protein G beads. For the FLAG-M2 (Sigma) IP, the nuclear extract was directly incubated with the resin for 2-3 hrs. Protein complexes were eluted from beads by boiling in 120 µl SDS-containing protein loading buffer. 10 µl was used for each immunoblot analysis with 5% input. IgG was used to demonstrate thorough washing.

ChIP Assay. Cells were grown to an approximate final count of $5x10^7$ – $1x10^8$ cells for each location analysis reaction. Cells were chemically cross-linked with 1% formaldehyde solution for 10 min at room temperature with gentle agitation and quenched with 0.125 M glycine. Cells were rinsed twice with 1xPBS, flashes frozen and stored at –80 °C. Cells were re-suspended, lysed, and sonicated to solubilize and shear crosslinked DNA. To ensure consistent sonication between samples, we used Bioruptor (Diagenode). Sonication was performed for 4-6 cycles (30 s-ON, 30 s-OFF). The resulting chromatin extract was precleared and appropriate amount was taken to incubate at 4 °C with 2-10 µg of antibody for at least 3 hr.

H2AK119ub1 ChIP. Cells cultured in 2i medium were trypsinized and followed by resuspension in PBS containing trypsin inhibitors. After spinning down the cells, the pellet were resuspended in cold CSK buffer (100 mM NaCl, 300mM sucrose, 3 mM

$MgCl_2$, 10 mM PIPES, pH 6.8) containing Triton X-100 (0.5%) and EGTA (1 mM) keeping in ice for 5 min. Buffer were then removed, replaced by 15 ml 0.5% formaldehyde solution, incubating for 10 minutes at room temperature and quenched by 1 ml 2 M Glycine (0.125 M final). Cells were then spun down, washed with cold PBS once, and the cell pellet were resuspended in Swelling buffer (25 mM Hepes pH 7.5, 1.5 mM $MgCl_2$, 10 mM KCl, 0.1% NP-40, 1 mM DTT, 2 mM PMSF, 1 μg/ml leupeptin, 1 μg/ml aprotinin), incubating on ice for 10min. To extract the nuclei, swollen cells were homogenized with Dounce homogenizer (pestle A) ~20times. After spinning down at 2000 rpm for 5~10 min, the nuclei were resuspended in Sonication buffer (50 mM HEPES pH 7.5, 140 mM NaCl, 1 mM EDTA, 1% Triton X-100, 0.1% Na-deoxycholate, 0.1% SDS, and 2 mM PMSF, 1 μg/ml leupeptin, 1 μg/ml aprotinin) and sonicated in Bioruptor (Diagenode) after keeping on ice for 20 min. Lysate were spun down for 15 min 13000 rpm at 4˚C and the supernatant were pre-cleared by 0.1% BSA pre-blocked goat anti-IgM beads (Sigma, A4540) and used for ChIP. IgM or H2AK119ub1 (E6C5, Millipore 05-678) (4 μg) antibody was added and rotated overnight in cold room. On the next morning, pre-blocked beads were added and rotated for another 3 hrs at 4˚C. Beads were then washed with Sonication buffer twice, Washing buffer (2 mM Tris pH 8.0, 0.02 mM EDTA, 50 mM LiCl, 0.1% NP-40 0.1% Na-deoxycholate) once, TE once, followed by reverse crosslink for 5 hrs at 65 °C.

FLAG-HA tandem ChIP. Solubilized chromatin fragments were diluted 4 times by IP150 buffer (50 mM Tris-HCl at pH 7.5, 150 mM NaCl, 5% glycerol, 0.2% Igepal [Sigma], Aprotein, Leupeptin, 100 mM PMSF, 1 mM DTT) to lower SDS concentration and then incubated with anti-FLAG M2-agarose (Sigma) for 3 hrs, washed three times for 2 min each time with IP300 buffer and eluted with 500 μg/ml FLAG peptide twice for 1 hr each at 4 °C. The eluted fragments were subsequently incubated with anti-HA agarose (Sigma) for 4 hrs, washed three times for 2 min each with IP300 buffer and eluted with ChIP elution buffer (50 mM Tris, 10 mM EDTA, PH 8.0, 1% (v/v) SDS) at 65 °C.

For all ChIP assays, DNA was purified using the QIAGEN PCR purification kit according to the manufacturer's protocol after the reverse crosslink. Relative occupancies

were calculated by determining the immunoprecipitation efficiency (ratios of the amount of immunoprecipitated DNA to that of the input sample).

ChIP Sequencing

Library Preparation. 5-10 ng of ChIP DNA was used for generation of libraries for deep-sequencing using the NEBNext DNA Sample Prep Master Mix. Briefly, the DNA was end-repaired following adding an A-base to the end-repaired DNA fragments. Illumina adaptors (regular or multiplex) were ligated to the ChIP DNA fragments and 200-400 bp of size fractions were excised from 2% agarose gel. Adaptor-modified fragments were enriched by 18 cycles of PCR amplification by mutiplex index primers. The DNA library prep was validated in Bioanalyzer for quantity and size before putting into sequencing.

ChIP-Seq Data Analysis. All fastq files including previously published samples were aligned to the Mouse reference genome (UCSC, mm9 assembly) using Bowtie allowing only uniquely mapping reads (settings: -p 20 -S -m 1). Peak detection was performed using the MACS version 2 software (Zhang et al., 2008) with default settings (except: "--broad --format=BAM -g mm"). The "--broad" parameters causes MACS to output both "normal" and "broad" peaks, where normal peaks are merged into broad peaks, if they are closely located on the same chromosome. All the succeeding analyses were based on broad peaks. IgG samples were used as peak calling controls. Chromosomal positions were annotated to the RefSeq database (mm9) using the UCSC refFlat table (Rhead et al., 2010). Genes not uniquely mapped to the genome were excluded and to avoid redundancy only the longest transcript of each gene was used. All chromosomal interval overlaps were performed using 'intersectBed' script from UCSC. To create a bigwig (i.e. wiggle format) file each mapped read was first extended in the 3'-direction to a total length of 250 bases (our estimated fragment length). The modified alignment file was then transformed to a bedGraph file, where densities were scaled according to millions of unique reads, before finally being converted to a bigwig file. All heatmaps and plots were generated using seqMINER (Ye et al., 2011). VENN-diagrams are based on number of unique genes containing one or more called peaks. The ChIP-seq data have been submitted to the GEO database (GSE37930).

SUPPLEMENTAL FIGURES

Figure S1

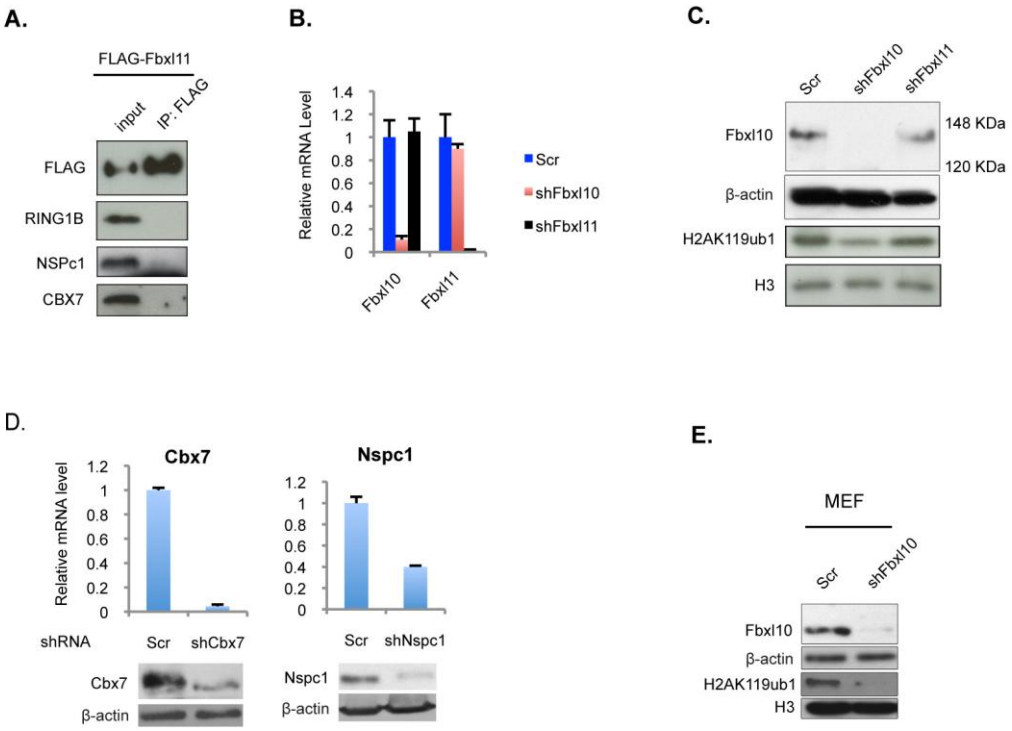

Figure S1 Fbxl11 Does Not Interact with PRC1 Proteins, and Depletion of Fbxl11 in ESCs Does Not Affect H2AK119 Monoubiquitylation, Related to Figure 1

(A) Anti-FLAG IP of FLAG-HA-Fbxl11 ectopically expressed in 293FT cells followed by WB using antibodies to the indicated proteins.

(B) Real-time qPCR showing that Fbxl10 or Fbxl11 is significantly and specifically depleted by the expressed shRNAs. The error bars denote s.d., n=2.

(C) Western blots showing that Fbxl10 or Fbxl11 is significantly depleted by the specific shRNAs, and that the Fbxl10 antibody does not cross-react with Fbxl11. WB for acid extracted histones shows that H2AK119ub1 levels remain constant upon the depletion of Fbxl11.

(D) Real-time qPCR and Western blots showing that Cbx7 and Nspc1 are significantly depleted by the indicated shRNAs. The error bars denote s.d., n=2.

(E) WB analysis showing that H2AK119Ub1 is significantly decreased upon loss of Fbxl10 in primary mouse embryonic fibroblasts (MEF). β-actin served as a loading control for total protein. H3 served as a loading control for histones.

Figure S2

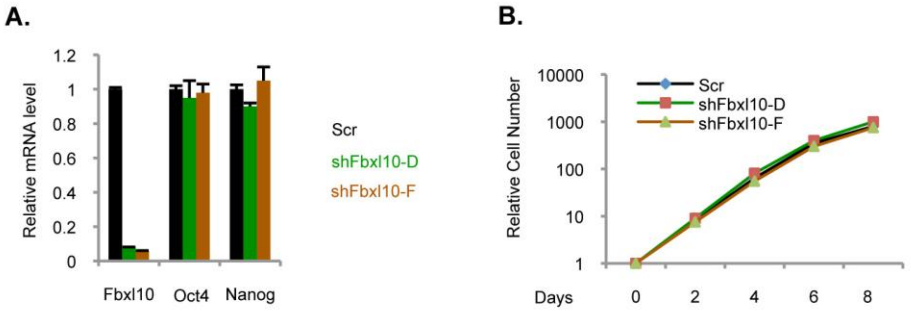

Figure S2. Depletion of Fbxl10 Does Not Affect the Expression of Pluripotent Transcription Factors or the Proliferation of Mouse ESCs, Related to Figure 1

(A) Real-time qPCR analyses showing mRNA levels of Fbxl10, Oct4 and Nanog in control (Scr) or Fbxl10-depleted ES cells (shFbxl10-D and shFbxl10-F). The error bars denote s.d., n=2.

(B) Growth curves indicating similar proliferation rates of control and Fbxl10-depleted ES cells.

Figure S3

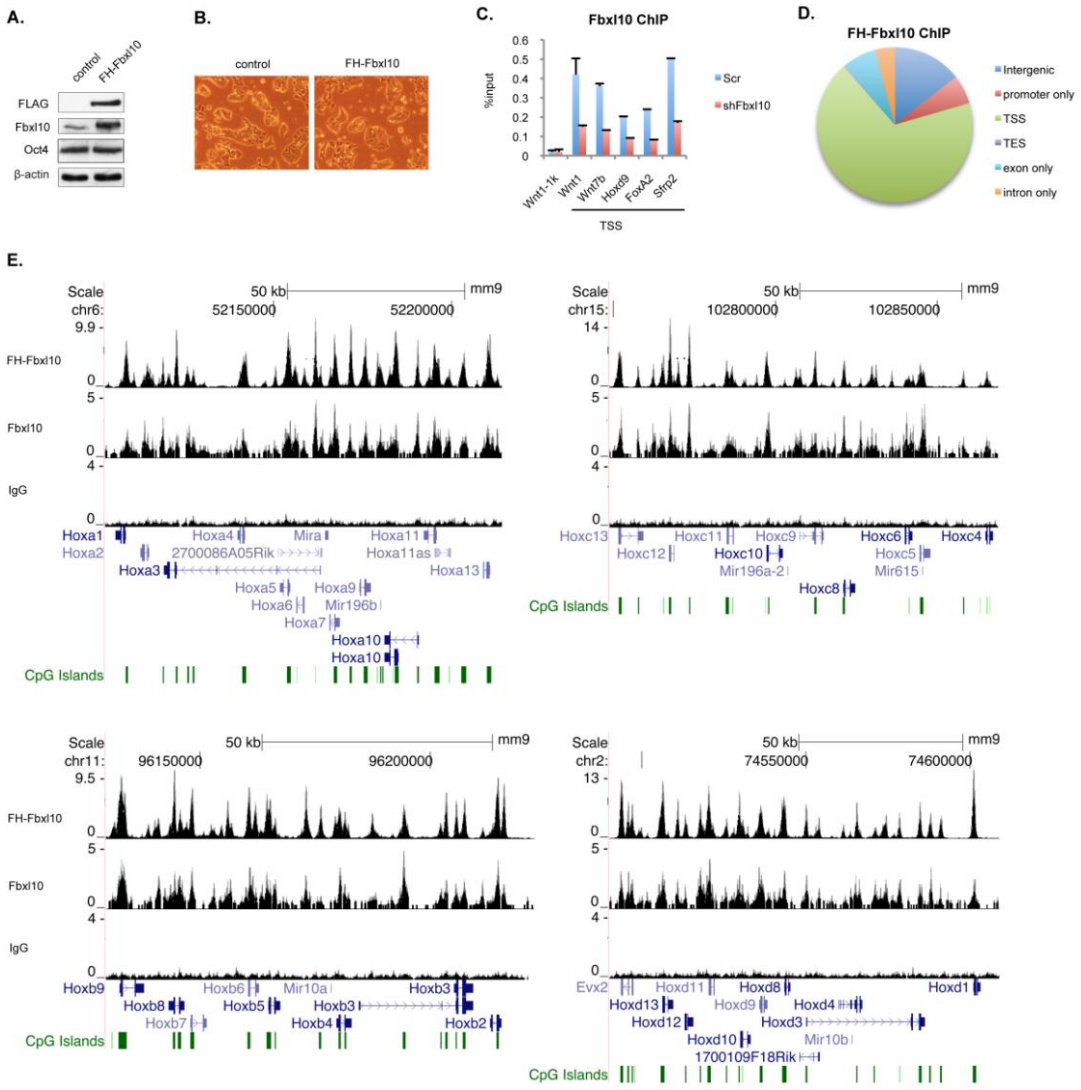

Figure S3. Fbxl10 Binds to CpG Islands, Related to Figure 3

(A) WB analysis of total protein lysate of control and FH-Fbxl10 stable ES cells. β-actin served as a loading control.

(B) Bright field pictures showing morphology of control and FH-Fbxl10 expressing ESCs. Original magnification ×10.

(C) Fbxl10 ChIP-qPCR analyses in control (Scr) and Fbxl10-depleted (shFbxl10-D) ES cells. *Wnt1*-1 kb without CpG rich sequences served as a negative control for the target sites. The error bars denote s.d., n=3.

(D) Diagram illustrating the overall distribution of Fbxl10 binding sites into designated regions.

(E) FH-Fbxl10, Fbxl10 and IgG ChIP-seq profiles on the *Hoxa/b/c/d* clusters. The normalized number of tags (TPM) for each ChIP-seq is given to the left of each graph. CpG-islands are represented by green bars.

Figure S4

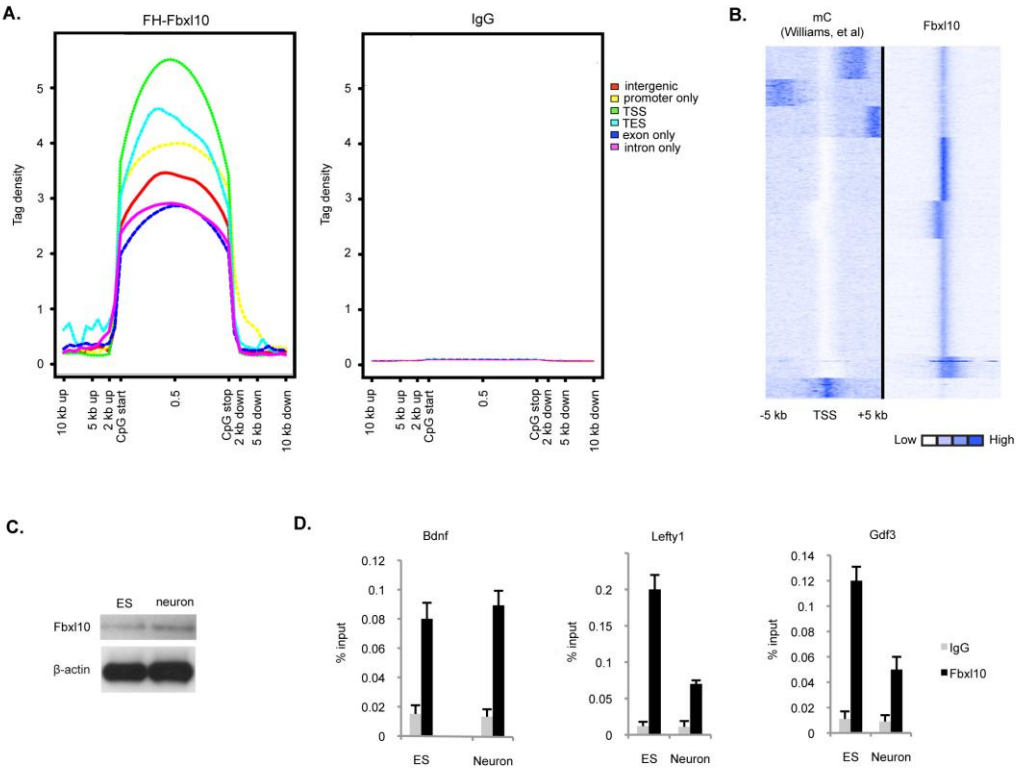

Figure S4. Fbxl10 Dynamically Binds to Unmethylated CpG Islands, Related to Figure 3

(A) Fbxl10 is specifically enriched over CpG islands irrespective of where they are located. Average FH-Fbxl10 and IgG tag density across CpG islands at TSS (green line), transcription end sites (TES) (light blue line), promoter only regions (yellow line), exon and intron only regions (blue and purple line) and intergenic regions (red line). The average read density across CpG islands 40 windows were created. Each CpG island was divided into 20 windows of equal size along with 10 upstream and downstream flanking windows with fixed individual length of 1 kb.

(B) Fbxl10 and mC are inversely correlated. Heat map shows Fbxl10 and mC profiles in a ±5 kb window centered around TSS of all Refseq genes.

(C) WB analysis showing that Fbxl10 expression is not decreased when ES cells are differentiated to neurons. β-actin served as a loading control.

(D) Fbxl10 is displaced, when the genes are DNA methylated. Fbxl10 ChIP-qPCR analyses were performed on target genes (*Lefty1* and *Gdf3*) known to be methylated in neurons. *Bdnf* promoter served as a negative control. The error bars denote s.d., n=2.

Figure S5

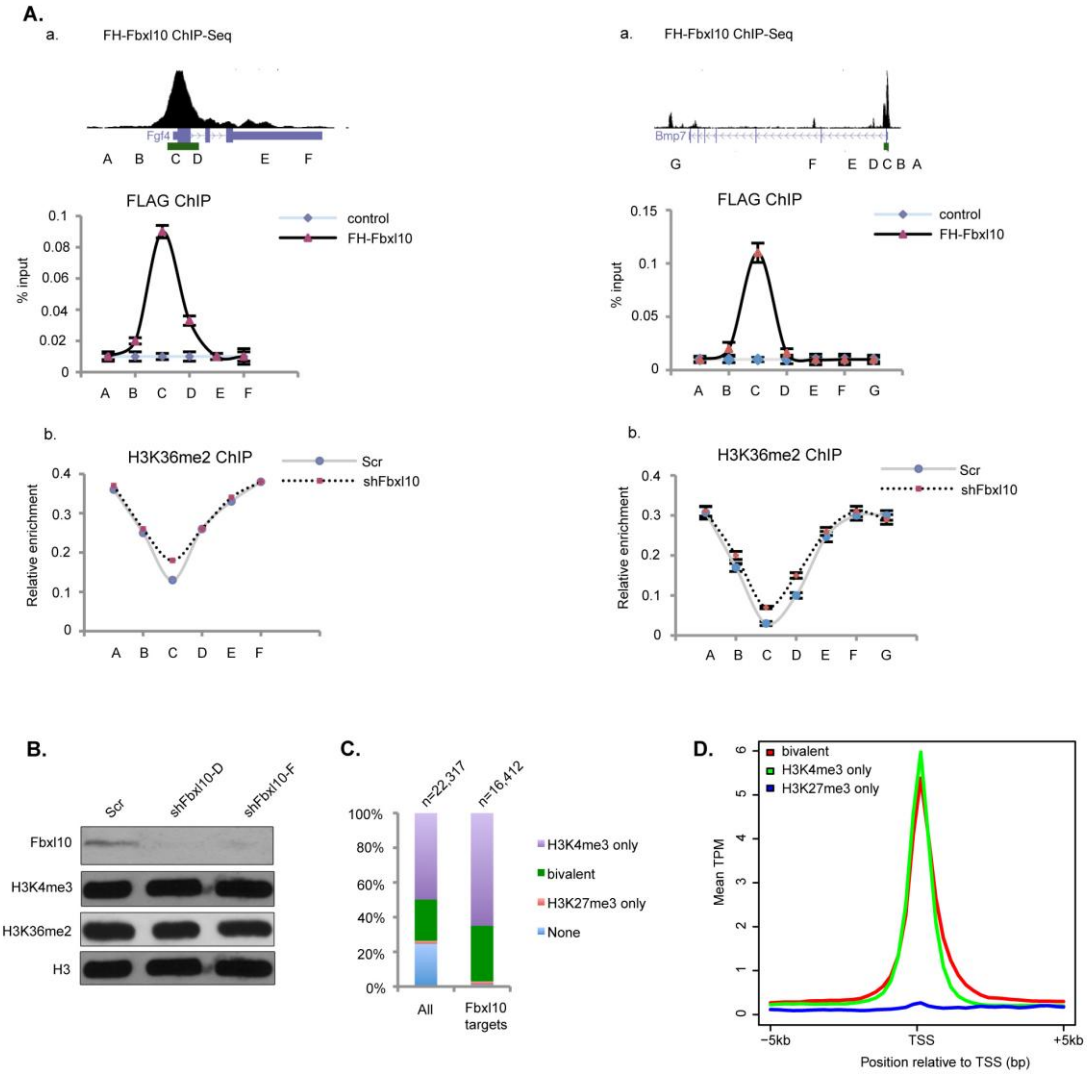

Figure S5. Fbxl10 Correlation with Histone Modification Profiles, Related to Figures 3 and 4

(A) Comparison of FH-Fbxl10 (upper panel a) and H3K36me2 (lower panel b) ChIP profiles across tiled CpG island genes, indicating specific enrichment of Fbxl10 and depletion of H3K36me2 at CpG islands. The H3K36me2 level is slightly increased upon loss of Fbxl10. FLAG ChIP was performed in control and FH-Fbxl10 stable ES cells. H3K36me2 ChIP was performed in control (Scr) and Fbxl10-depleted ES cells (shFbxl10). Relative enrichment values for H3K36me2 are normalized by histone H3 occupancy. The error bars denote s.d., n=2.

(B) Western blot showing that the global levels of H3K4me3 and H3K36me2 remain unchanged upon down-regulation of Fbxl10.
(C) Histograms showing distribution of H3K4me3 and/or H3K27me3 for all genes or FH-Fbxl10 target genes.
(D) Profiles of the mean ChIP-Seq signals of FH-Fbxl10 around TSS for H3K4me3-only, H3K27me3-only or bivalent genes. Densities (TPM) within ±5 kb regions relative to TSS were extracted from normalized bigwig files.

Figure S6

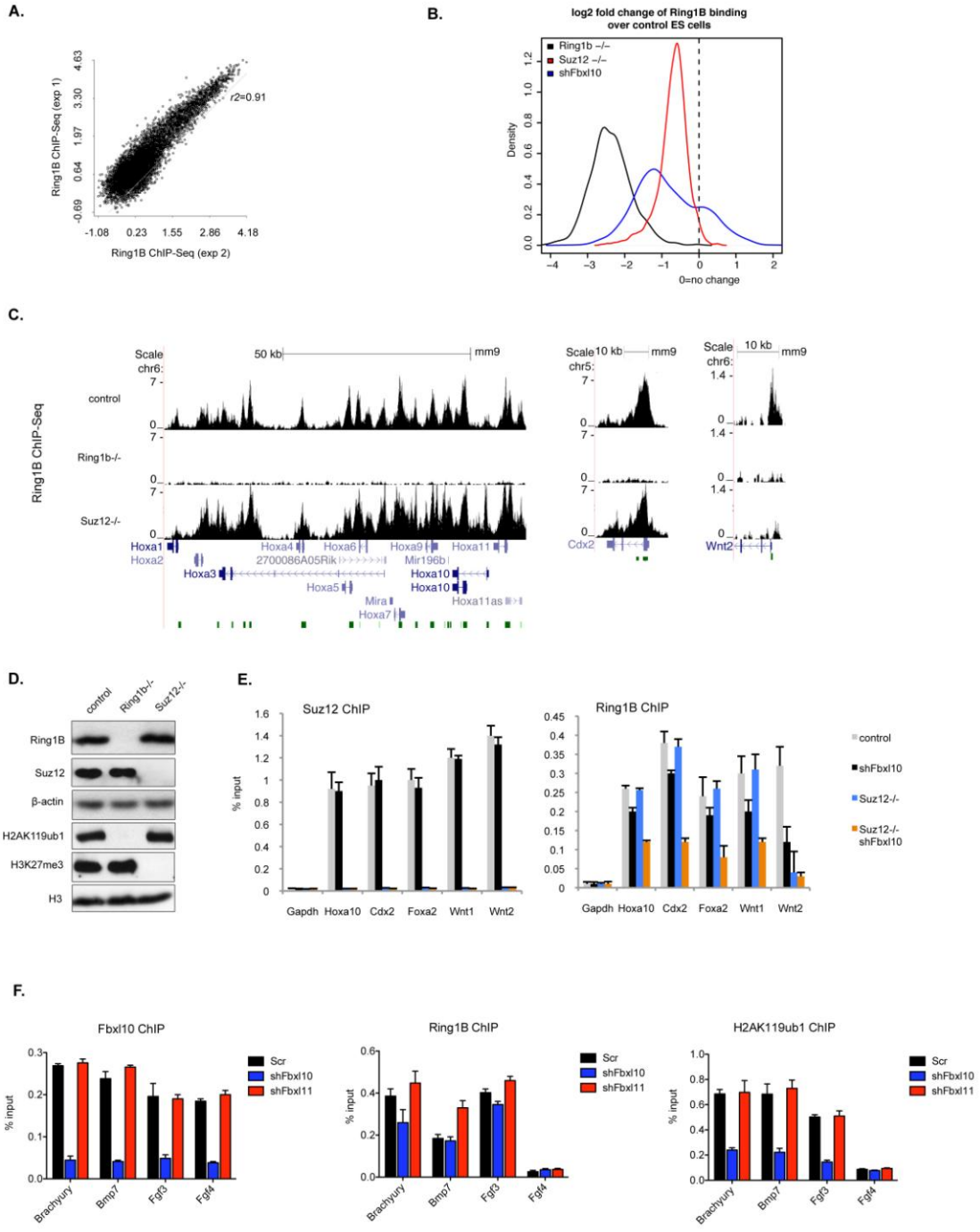
A.
Ring1B ChIP-Seq (exp 1)
Ring1B ChIP-Seq (exp 2)
r2=0.91
B.
log2 fold change of Ring1B binding over control ES cells
Ring1b −/−
Suz12 −/−
shFbxl10
Density
0=no change
C.
Ring1B ChIP-Seq
control
Ring1b-/-
Suz12-/-
50 kb
mm9
Hoxa1
Hoxa2
Hoxa3
Hoxa4
Hoxa5
Hoxa6
Hoxa7
Hoxa9
Hoxa10
Hoxa11
Hoxa11as
2700086A05Rik
Mir196b
Mira
Cdx2
Wnt2
D.
control
Ring1b-/-
Suz12-/-
Ring1B
Suz12
β-actin
H2AK119ub1
H3K27me3
H3
E.
Suz12 ChIP
Ring1B ChIP
% input
Gapdh
Hoxa10
Cdx2
Foxa2
Wnt1
Wnt2
control
shFbxl10
Suz12-/-
Suz12-/- shFbxl10
F.
Fbxl10 ChIP
Ring1B ChIP
H2AK119ub1 ChIP
% input
Scr
shFbxl10
shFbxl11
Brachyury
Bmp7
Fgf3
Fgf4

Figure S6. Fbxl10 Recruits Ring1B and Mediates H2AK119Ub1 Independent of PRC2, Related to Figure 5

(A) seqMINER derived dot-plot representing Ring1b (normalized) enrichment +/- 5kb around TSS of all RefSeq genes for two independet Ring1B ChIP-seq experiments. The experiments show high reproducibility with a Pearson's correlation coefficient of 0.91.

(B) Distribution of log2 fold change of Ring1B binding in *Ring1B-/-*, *Suz12-/-* and shFbxl10-ES cells over control ES cells on all Ring1B target sites (broad peaks identified by MACS2). The tag counts under each target peak were extracted from the normalized bigwig files. The x-axis represents the log2 ratio of Ring1B tag density between the designated cells and control cells. Negative fold change equals lower enrichment compared to control. A pseudo count (5% quantile) was added to all counts to avoid division by zero or highly inflated fold changes.

(C) Tracks of Ring1B ChIP-Seq binding profiles are shown as examples for WT, *Ring1B-/-*, and *Suz12-/-* ESCs. The normalized tag number of reads (TPM) for each ChIP-seq is given at the top left of each graph.

(D) Western blot showing that bulk H2AK119Ub1 is lost in *Ring1B-/-*, but not in *Suz12-/-* ESCs.

(E) ChIP-qPCR analyses showing that Fbxl10 recruits Ring1B independent of PRC2. Suz12 and Ring1B ChIP assays were performed in the indicated ESCs. The error bars denote s.d., n=3.

(F) ChIP-qPCR analyses showing depletion of Fbxl11 does not affect Fbxl10 binding, Ring1B recruitment and H2AK119 monoubiquitylation. The error bars denote s.d., n=2.

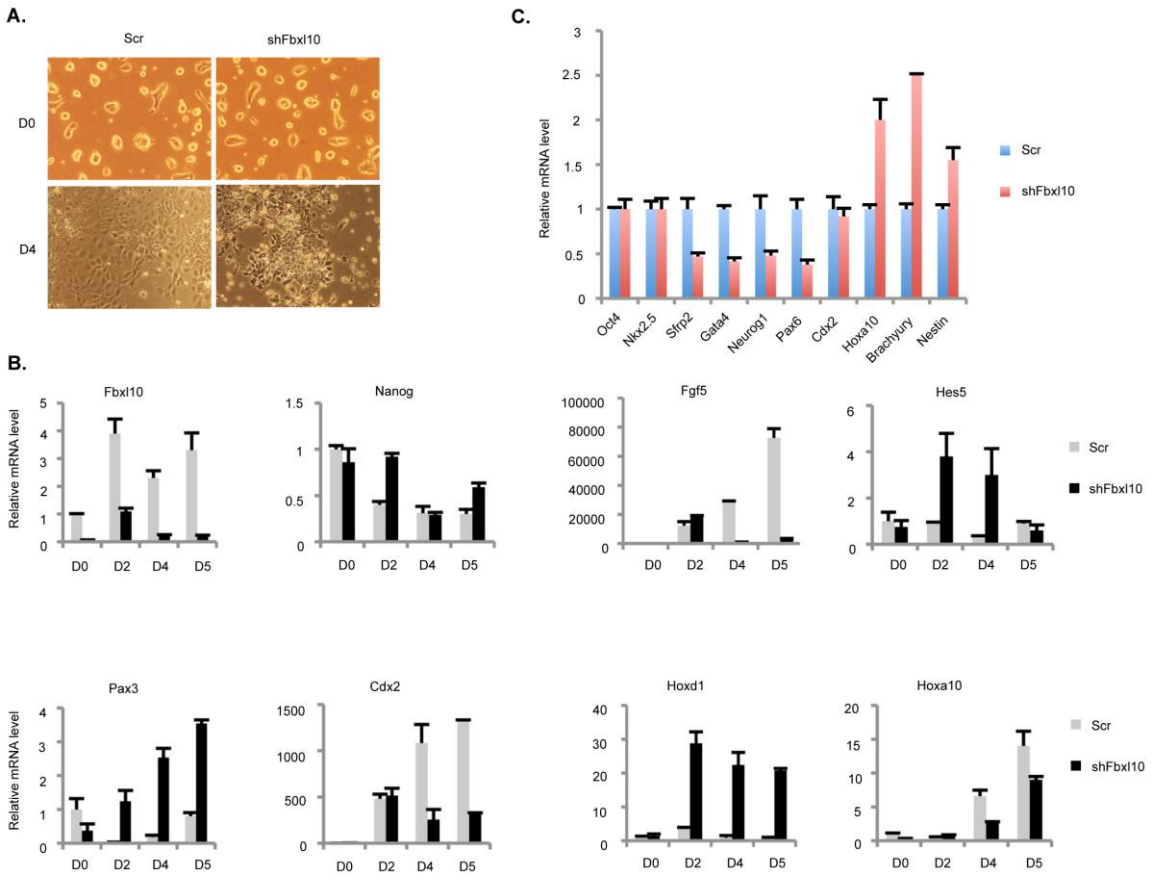

Figure S7. Fbxl10 Is Required for ESC Monolayer Differentiation, Related to Figure 7

(A) Monolayer differentiation of control (Scr) and Fbxl10-depleted (shFbxl10) ESCs. Bright field picture showing morphology of the ES cell lines at day 0 and day 4 of differentiation.

(B) Real-time qPCR analyses of the indicated genes during ESC differentiation of control (Scr) and Fbxl10-depleted (shFbxl10) ESCs on the indicated days of differentiation. The error bars denote s.d., n=2.

(C) Real-time qPCR analyses of lineage markers or representative Fbxl10 target genes in control (Scr) and Fbxl10-depleted (shFbxl10) ESCs. The error bars denote s.d., n=3.

SUPPLEMENTAL REFERENCES

Blackledge et al., CpG islands recruit a histone H3 lysine 36 demethylase. Mol Cell (2010); 38(2): 179-90.

Brookes, E., de Santiago, I., Hebenstreit, D., Morris, K.J., Carroll, T., Xie, S.Q.,, *et al.* (2012). Polycomb Associates Genome-wide with a Specific RNA Polymerase II Variant, and Regulates Metabolic Genes in ESCs. Cell stem cell *10*, 157-170.

Hansen, K.H., Bracken, A.P., Pasini, D., Dietrich, N., Gehani, S.S., Monrad, A., Rappsilber, J., Lerdrup, M., and Helin, K. (2008). A model for transmission of the H3K27me3 epigenetic mark. Nature Cell Biology *10*, 1291-1300.

Lienert, F., Mohn, F., Tiwari, V.K., Baubec, T., Roloff, T.C., Gaidatzis, D., Stadler, M.B., and Schubeler, D. (2011a). Genomic prevalence of heterochromatic H3K9me2 and transcription do not discriminate pluripotent from terminally differentiated cells. PLoS genetics *7*, e1002090.

Lienert, F., Wirbelauer, C., Som, I., Dean, A., Mohn, F., and Schubeler, D. (2011b). Identification of genetic elements that autonomously determine DNA methylation states. Nature genetics *43*, 1091-1097.

Marson, A., Levine, S.S., Cole, M.F., Frampton, G.M., Brambrink, T., *et al.* (2008). Connecting microRNA genes to the core transcriptional regulatory circuitry of embryonic stem cells. Cell *134*, 521-533.

Pasini, D., Bracken, A.P., Hansen, J.B., Capillo, M., and Helin, K. (2007). The polycomb group protein Suz12 is required for embryonic stem cell differentiation. Molecular and Cellular Biology *27*, 3769-3779.

Pasini, D., Hansen, K.H., Christensen, J., Agger, K., Cloos, P.A., and Helin, K. (2008). Coordinated regulation of transcriptional repression by the RBP2 H3K4 demethylase and Polycomb-Repressive Complex 2. Genes & Development *22*, 1345-1355.

Rhead, B., Karolchik, D., Kuhn, R.M., Hinrichs, A.S., Zweig, A.S., Fujita, P.A., Diekhans, M., Smith, K.E., Rosenbloom, K.R., Raney, B.J., *et al.* (2010). The UCSC Genome Browser database: update 2010. Nucleic Acids Research *38*, D613-619.

Schmitz, S.U., Albert, M., Malatesta, M., Morey, L., Johansen, J.V., Bak, M., Tommerup, N., Abarrategui, I., and Helin, K. (2011). Jarid1b targets genes regulating development and is involved in neural differentiation. The EMBO journal *30*, 4586-4600.

Ye, T., Krebs, A.R., Choukrallah, M.A., Keime, C., Plewniak, F., Davidson, I., and Tora, L. (2011). seqMINER: an integrated ChIP-seq data interpretation platform. Nucleic Acids Research *39*, e35.

Zhang, Y., Liu, T., Meyer, C.A., Eeckhoute, J., Johnson, D.S., Bernstein, B.E., Nusbaum, C., Myers, R.M., Brown, M., Li, W., *et al.* (2008). Model-based analysis of ChIP-Seq (MACS). Genome Biology *9*, R137.